Reentry Trajectory Optimization of Variable-Configuration Hypersonic Glide Vehicle

*LI Chang, ZHAO Jisong**

College of Astronautics, Nanjing University of Aeronautics and Astronautics, Nanjing 211106, P.R. China

(Received 23 June 2023; revised 7 September 2023; accepted 1 October 2023)

Abstract: The reentry trajectory optimization of a variable-configuration vehicle (VCV) is studied. A surrogate model is established for quick prediction of vehicle aerodynamics at different deformation and flight conditions. The time histories of deformation, angle of attack and bank angle are all taken as trajectory optimization variables, and the performance of the VCV in landing coverage area and the maneuverability to avoid obstacles are quantitatively studied. Simulation results show that compared with the fixed-configuration vehicle (FCV), the VCV can achieve the optimal morphing in addition to the optimal control along the reentry glide trajectory, thus leading to better reentry trajectory performance.

Key words: hypersonic glide; aerodynamic surrogate model; trajectory optimization; variable-configuration

CLC number: V448 **Document code:** A **Article ID:** 1005-1120(2023)S2-0032-08

0 Introduction

Hypersonic vehicle technology is one of the most advanced technologies in the field of aerospace. From the perspective of foreign investment, hypersonic glide vehicle will become the focus of hypersonic research[1]. The aerodynamic configuration of the existing glide vehicle is designed for specific operating points, and the maximum lift-drag ratio can be achieved only under the specific flight condition, which makes it difficult to exert the potential of the vehicle. The application of morphing technology on hypersonic glide vehicle can consider the flight performance requirements in all design stages and enhance the environmental adaptability of the vehicle[2].

The trajectory optimization of a hypersonic reentry vehicle is an extremely complex optimal control problem with strong nonlinearity and multiple constraints. The control variables expand more dimensions on the original basis, which makes the solution more difficult under the joint optimization. Based on the trajectory optimization of morphing glide vehicle, Chen et al.[3] established a model with redundant control variables and quantified the performance of the telescopic morphing glide vehicle by using the pseudo-spectral method. Yang et al.[4] designed a fold-wing aircraft and used Gauss pseudo-spectral method to optimize the glide trajectory of fixed-wing aircraft and fold-wing aircraft respectively. Zhu et al.[5] adjusted the deformation of a lifting body vehicle as the additional control variable to effectively expand the flight strategy of vehicle. Huang et al.[6] studied the tactical missile based on variable-sweep wing airfoil and used Radau pseudo-spectral method (RPM) to optimize the trajectory of variable-sweep wing airfoil and fixed-wing airfoil respectively. Peng et al.[7] adopt multi-objective optimization algorithm for glide trajectory of telescopic wing aircraft and obtained Pareto Front with relatively uniform distribution. Wang et al.[8] adopt the bivariate optimization scheme of sweep angle and angle of attack to optimize the trajectory of the morphing-wing missile by hp-adaptive RPM.

In this paper, the trajectory optimization of hy-

*Corresponding author, E-mail address: zhaojisong@nuaa.edu.cn.

How to cite this article: LI Chang, ZHAO Jisong. Reentry trajectory optimization of variable-configuration hypersonic glide vehicle[J]. Transactions of Nanjing University of Aeronautics and Astronautics, 2023, 40(S2): 32-39.

http://dx.doi.org/10.16356/j.1005-1120.2023.S2.005

personic glide vehicle with variable wingspan is studied. In particularly, the deformation of wingspan is also extended as a control variable in addition to the angle of attack and the bank angle. An aerodynamic surrogate model based on BP neural network (BPNN) is constructed by the aerodynamic integration design platform. The configuration and trajectory of the variable-configuration vehicle (VCV) are jointly optimized by the hp-adaptive RPM to improve the performance, and the optimal deformation and control along the reentry trajectory can be obtained.

1 Vehicle Reference Configuration and Morphing Model

The baseline configuration of the VCV is shown in Fig.1.

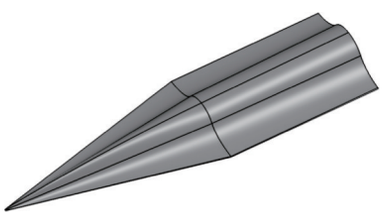

Fig.1 Basic configuration of the VCV

The morphing of the VCV is achieved by adjusting the wingspan W. The configurations of a minimum wingspan and a maximum wingspan are shown in Fig.2 and Fig.3.

Fig.2 Minimum wingspan configuration

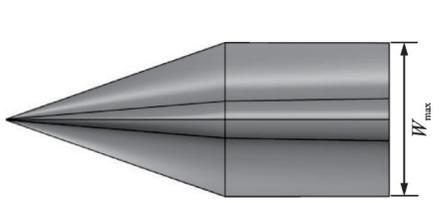

Fig.3 Maximum wingspan configuration

2 Trajectory Optimization Model

2.1 Model of dynamics

Assuming that the Earth is a uniform sphere without rotation, the dynamics equations are as follows[9]

$$\begin{cases} \dot{r} = v\sin\gamma \\ \dot{\theta} = \dfrac{v\cos\gamma\sin\psi}{r\cos\varphi} \\ \dot{\varphi} = \dfrac{v\cos\gamma\cos\psi}{r} \\ \dot{v} = -\dfrac{D}{m} - g\sin\gamma \\ \dot{\gamma} = \dfrac{L\cos\sigma}{mv} - \dfrac{g\cos\gamma}{v} + \dfrac{v\cos\gamma}{r} \\ \dot{\psi} = \dfrac{L\sin\sigma}{mv\cos\gamma} + \dfrac{v}{r}\cos\gamma\sin\psi\tan\varphi \end{cases} \tag{1}$$

where r is the radial distance from the Earth center to the vehicle, v the velocity of the vehicle, γ the flight path angle between the velocity and the local horizontal plane, ψ the heading angle between the projection of the velocity on the horizontal plane and the North, and m the mass of the vehicle; θ and φ are the longitude and latitude, and L and D the aerodynamic lift and drag. The acceleration of gravity is $g = \mu / r^2$, where μ is the gravitational constant for the Earth with value of $3.986\,031\,95\times10^{14}$ m^3/s^2.

2.2 Constraints

Hypersonic glide vehicle is subject to various constraints. The endpoint constraints, path constraints and control variables are considered in this paper.

Endpoint constraints include initial constraints and terminal constraints

$$\boldsymbol{x}(t_0) = \boldsymbol{x}_0 \tag{2}$$

$$\boldsymbol{x}(t_f) = \boldsymbol{x}_f \tag{3}$$

where $\boldsymbol{x}_0$ is the initial state variable and $\boldsymbol{x}_f$ the terminal state variable. Here, $\boldsymbol{x} = [r\ \theta\ \varphi\ v\ \gamma\ \psi]^{\mathrm{T}}$.

Path constraints mainly include

$$q = \frac{1}{2}\rho v^2 \leqslant q_{\max} \tag{4}$$

$$\dot{Q} = k_Q \rho^{0.5} v^{3.15} \leqslant \dot{Q}_{\max} \tag{5}$$

$$N = \frac{\sqrt{L^2 + D^2}}{mg} \leqslant N_{\max} \tag{6}$$

where q is the dynamic pressure, $q_{\max}$ the maximum allowed dynamic pressure, $\dot{Q}$ the stagnation point heat flux density, $\dot{Q}_{\max}$ the maximum allowed heat flux density, N the overload, and $N_{\max}$ the maximum allowable overload. In these equations, k_Q is

an empirical constant related to the vehicle nose radius, and ρ the atmospheric density. The 1976 U.S. Standard Atmosphere[10] is used in this paper.

The following control constraints are considered

$$\alpha_{\min} \leqslant \alpha(t) \leqslant \alpha_{\max} \tag{7}$$

$$\sigma_{\min} \leqslant \sigma(t) \leqslant \sigma_{\max} \tag{8}$$

$$W_{\min} \leqslant W(t) \leqslant W_{\max} \tag{9}$$

$$u_{\min} \leqslant \frac{\mathrm{d}\alpha(t)}{\mathrm{d}t} \leqslant u_{\max} \tag{10}$$

$$w_{\min} \leqslant \frac{\mathrm{d}w(t)}{\mathrm{d}t} \leqslant w_{\max} \tag{11}$$

where $\alpha_{\min}$ and $\alpha_{\max}$ are the lower limit and upper limit of the angle of attack, $\sigma_{\min}$ and $\sigma_{\max}$ the lower limit and upper limit of the bank angle, $W_{\min}$ and $W_{\max}$ the lower limit and upper limit of the wingspan, $u_{\min}$ and $u_{\max}$ the lower limit and upper limit of the angular rate, $w_{\min}$ and $w_{\max}$ the lower limit and upper limit of the deformation rate.

The state dynamics of Eq.(1) and the constraint described by Eqs.(2—9) can be discretized by the standard RPM. The control rate constraints given in Eq.(10) and Eq.(11) are treated in a direct manner. Taking Eq.(11) as an example, it can be discretized in the following manner

$$u_{\min} \leqslant \frac{\alpha_{k+1} - \alpha_k}{\Delta\tau_k (t_f - t_0)} \leqslant u_{\max} \tag{12}$$

where τ is the scaled time ranged between -1 and 1, $\Delta\tau_k = \tau_{k+1} - \tau_k$, and the set $\{\tau_k\}$ is the discretization points.

The constraint of Eq.(12) can be further converted into the following standard form

$$\alpha_k - \alpha_{k+1} - \Delta\tau_k u_{\min} t_0 + \Delta\tau_k u_{\min} t_f \leqslant 0 \tag{13}$$

$$-\alpha_k + \alpha_{k+1} + \Delta\tau_k u_{\max} t_0 - \Delta\tau_k u_{\max} t_f \leqslant 0 \tag{14}$$

2.3 Surrogate model

The aerodynamic model of the VCV is a function of the angle of attack, Mach number and wingspan. Based on the Isight rapid integration and coupling of various softwares required for computational fluid dynmics (CFD) simulation, all the design processes are organized into a framework to complete the construction of the aerodynamic integrated design platform.

The experiment design method is adopted in Isight, and different values of each variable are selected to generate a sampling matrix. The sample conditions are shown in Table 1. Firstly, the sampling matrix outputs the geometry parameters to CATIA. The vehicle model is updated after receiving the new parameters. Then, the grids are generated automatically for the new vehicle geometry in Pointwise. Finally, according to the given simulation conditions, the CFD solution is solved by Fluent, and the aerodynamic data can be obtained.

Table 1 Calculation condition

Variable	Data point
Ma	{3, 5, 8, 10, 15, 20}
α / (°)	{−10, −7, −5, −3, 1, 3, 5, 7, 9, 11, 13, 15, 17, 20}
W / mm	{1 200, 1 600, 2 000, 2 400}

BPNN is one of the most representative algorithms in artificial neural network with good generalization in addition to fault tolerance and self-adaptability[11]. In this paper, the wingspan W, Mach number Ma and the angle of attack α are taken as input parameters, and the lift coefficient C_L and drag coefficient C_D are taken as output parameters. An example of the surrogate model based on BPNN is shown in Fig.4.

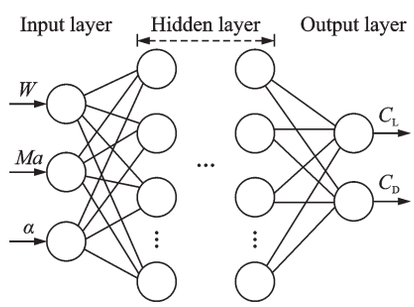

Fig.4 Structure of BPNN surrogate model

The mean squared error (MSE) is used to represent the accuracy of the surrogate model. A smaller value of MSE indicates higher accuracy in prediction of aerodynamic data. The MSE of the surrogate model is shown in Fig.5.

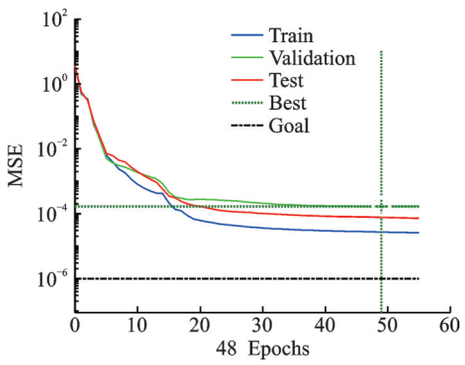

Fig.5 MSE of the surrogate

3 Joint Optimization and Performance Analysis

3.1 Simulation parameter

The simulation parameters of the trajectory optimization problem of VCV are shown in Table 2.

Table 2 Simulation parameters

Parameter	Value
h_0 / km	70
θ_0 / (°)	0
φ_0 / (°)	0
v_0 / (m•s^{-1})	5 500
γ_0 / (°)	0
ψ_0 / (°)	90
h_f / km	20
v_f / (m•s^{-1})	1 000
α / (°)	[10, 20]
σ / (°)	[−90, 90]
W / mm	[1 200, 2 400]
u / ((°)•s^{-1})	[−1/30, 1/30]
w / (mm•s^{-1})	[−1, 1]
q / kPa	⩽ 200
n	⩽ 4
$\dot{Q}$/ (kW•m^{-2})	⩽ 2 000

3.2 Trajectory optimization method

Currently, most of the numerical methods for trajectory optimization can be divided into two basic types: Indirect method and direct method. As a representative method of direct method, RPM uses Legendre-Gauss-Radau (LGR) points in the interval [−1, 1) to discretize state variables and control variables. To approximate the state variables and control variables, discrete points are used to construct Lagrange interpolation polynomials[12]. The differential equations are transformed into a set of algebraic constraints by taking the derivative of the global interpolation polynomial to approximate the derivative of the state variable with respect to time. After the transformation, the optimal control problem can be transformed into a set of algebraic constraint parameter optimization problems, which can then be solved by the nonlinear programming (NLP) method[13].

Finite element method (FEM) is a numerical method to solve mechanical problems by discretizing continuous objects. The hp-type FEM combines the advantages of h-type FEM and p-type FEM, allowing the element length h and basic function order p to be changed simultaneously and independently[14].

The hp-adaptive RPM combines the idea of FEM with RPM and applies the NLP method to solve the corresponding problems. The hp-adaptive algorithm can increase the order of the global interpolation polynomial or the number of time section for updating the NLP problem when the results do not meet the accuracy requirements[15]. In this paper, GPOPS-Ⅱ is employed to solve the trajectory optimization by using the hp-adaptive RPM[16].

3.3 Maximum longitudinal range trajectory

The hp-adaptive RPM is used to optimize the maximum longitudinal range trajectories of the VCV and the fixed-configuration vehile (FCV) with a wingspan of 1 600 mm. The results are shown in Figs.6—8.

As shown in Fig.6, the maximum longitudinal range of the VCV is 124.7° (corresponding to 13 843.5 km), and that of the FCV is 102.4° (11 367.9 km). Compared with the FCV, the longitudinal range of the VCV is increased by 21.8%.

Fig.7 shows that the VCV generally glides at the maximum wingspan in the reentry stage and requires a smaller value of the angle of attack.

It can be seen from Fig.8 that the peak dynamic pressure and heat flux of the VCV are smaller than

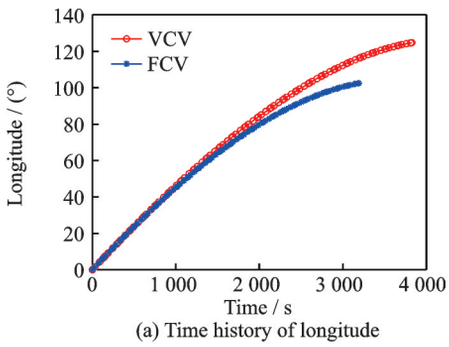

(a) Time history of longitude

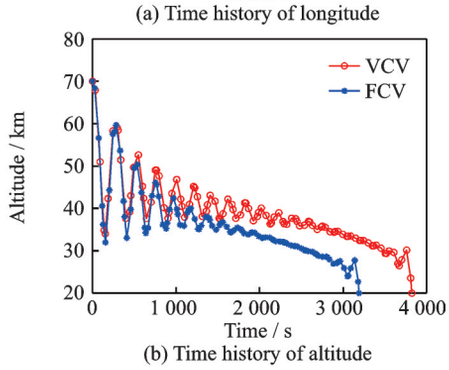

(b) Time history of altitude

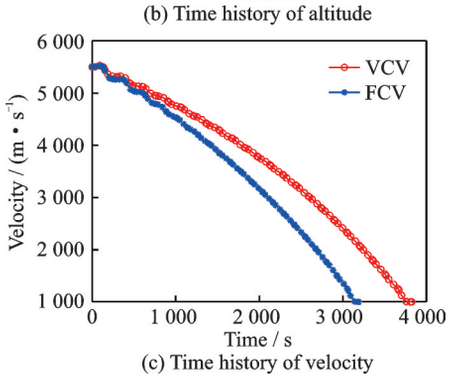

(c) Time history of velocity

Fig.6 Time histories of state variables

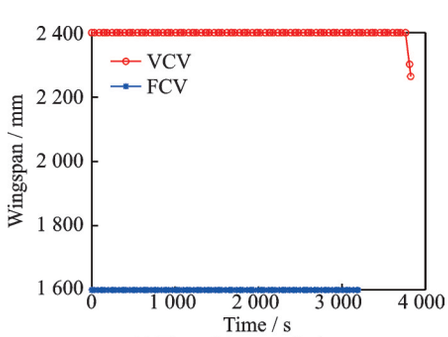

(a) Times history of wingspan

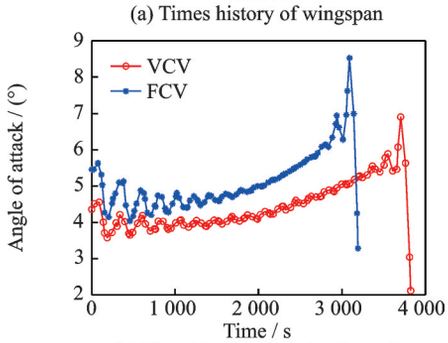

(b) Time history of angle of attack

Fig.7 Time histories of control variables of the maximum longitudinal range trajectory

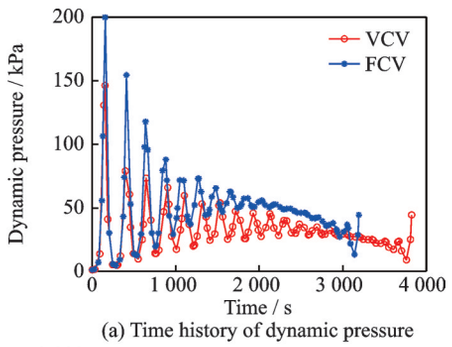

(a) Time history of dynamic pressure

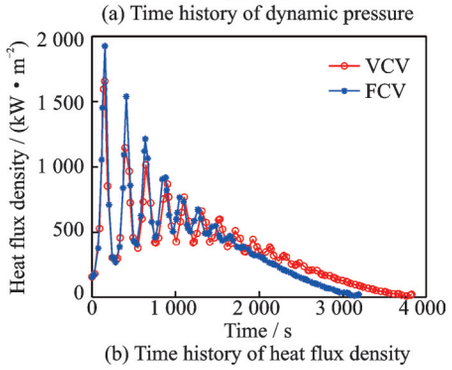

(b) Time history of heat flux density

Fig.8 Time histories of path constraints

those of the FCV. So the VCV is helpful to reduce the heating rate.

3.4 Minimum longitudinal range trajectory

The minimum longitudinal trajectory can reflect the maneuvering ability of the vehicle, and it is also a vital indicator to determine the range of landing coverage area. Simulation results are shown in Figs.9—11.

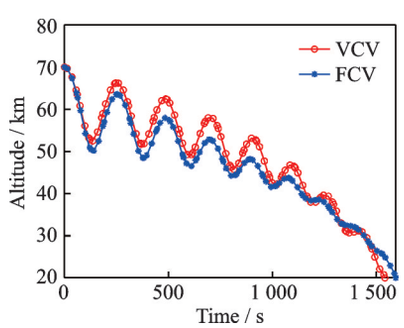

Fig.9 Time history of altitude

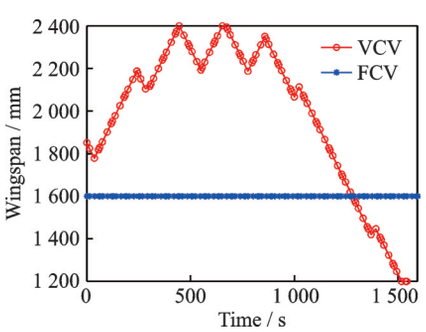

Fig.10 Time history of wingspan

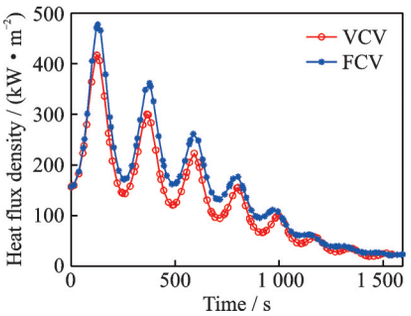

Fig.11 Time history of heat flux density

The trajectory of the VCV makes high frequency fluctuations in higher airspace, which increases the difficulty of intercepting weapons tracking and hitting. Since the VCV spends most of its time gliding in airspace with low atmospheric density, which ensures the reliability of the deformation mechanism.

3.5 Landing coverage area

The simulation result is shown in Fig.12. Because the Earth's rotation is neglected, the landing coverage area is symmetrically distributed. In Fig.12, the outer envelope is the landing coverage area of the VCV, and the inner is the FCV's. The result shows that the landing coverage area of the VCV increases by 94.7% compared with that of the FCV.

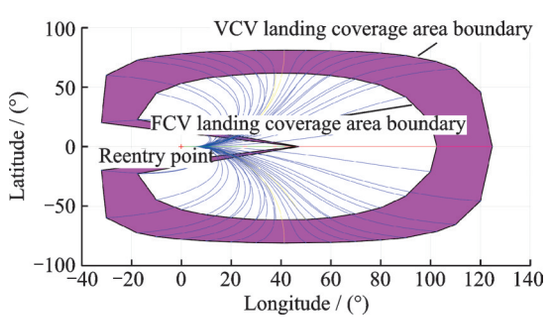

Fig.12 Landing coverage area

3.6 Maneuverability to avoid obstacles

It is assumed that the position of the reentry point is at (0°, 0°). There are two circular no-fly zones along the trajectory. The first no-fly zone is located at (30°, 2°) with a radius of 500 km. The second no-fly zone is located at (50°, 3°) with a radius of 1 000 km. The position of the target point is (65°, 10°). Taking the shortest time to reach the target point as the objective function, the results are shown in Figs.13—14.

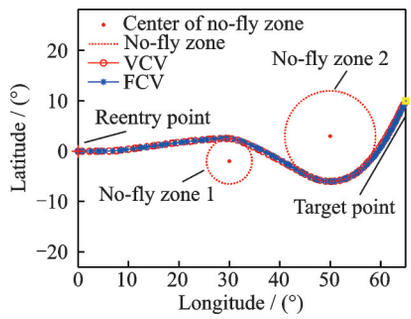

Fig.13 Maneuverability to avoid no-fly zones

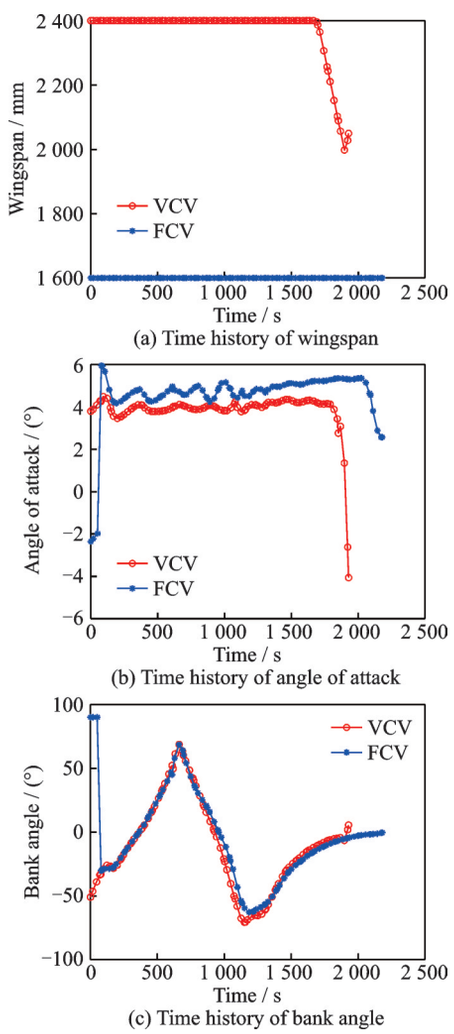

Fig.14 Time histories of control variables of maneuverability to avoid no-fly zones

It can be seen from Figs.13 and 14 that under the same reentry condition, the VCV can reach the target point in a relatively short time while avoiding the no-fly zones.

4 Conclusions

The reentry trajectory optimization of a hypersonic glide vehicle with the variable wingspan is

studied. The performance of the VCV in the landing coverage area and the maneuverability to avoid no-fly zones are quantitatively studied using the hp-adaptive RPM. Simulation results show that compared with the FCV with large lift-to-drag ratio, the maximum longitudinal range of the VCV is increased by 21.8%, and the landing coverage area is increased by 94.7%. The VCV can avoid no-fly zones in a short time by proper deformation. The trajectory optimization is carried out by considering the deformation of the vehicle wingspan, which can provide references for further design in this area.

References

[1] WANG Z D, WANG H, DING N, et al. Research on the development of hypersonic vehicle technology [J]. Science & Technology Review, 2021, 39(11): 59-67.

[2] CHEN T B, WANG H B, KANG Y L, et al. Application prospects of morphing technology in the boost-glide vehicle[J]. Tactical Missile Technology, 2017, 5(11): 1-5.

[3] CHEN T B, GONG M, WANG H B, et al. Trajectory optimization and performance analysis of the near-space morphing glide vehicles[J]. Journal of Astronautics, 2018, 39(9): 944-952.

[4] YANG B, ZHU Y C, WEI Y M, et al. Trajectory optimization and control analysis of folding wing aircraft[J]. Chinese Space Science and Technology, 2020, 40(3): 64-75.

[5] ZHU R Y, QI Z, WANG L S, et al. Trajectory optimization design of morphing vehicle[J]. Tactical Missile Technology, 2020, 5: 157-164.

[6] HUANG M H, TANG Q G, ZHANG Q B, et al. Morphing swept wing tactical missile conceptual design and optimization trajectory of hypersonic vehicle [J]. Tactical Missile Technology, 2016, 5(24): 10-17.

[7] PENG W Y, YANG T, WANG C Y, et al. Trajectory multi-objective optimization for hypersonic telescopic wing morphing aircraft[J]. Journal of National University of Defense Technology, 2019, 41(1): 41-47.

[8] WANG N, CHEN J Q, MING C, et al. Optimization design for trajectory of morphing-wing missile based on hp-adaptive pseudo-spectral method[J]. Journal of Ballistics, 2016, 28(4): 24-29.

[9] WU Xuzhong. Research on entry guidance and control algorithm for glide vehicle[D]. Beijing: Beijing Institute of Technology, 2014. (in Chinese)

[10] The COESA Working Group. US standard atmosphere (1976)[S]. Boulder: National Oceanographic and Atmospheric Administration, 1976.

[11] YUAN Yixin. Evolutionary algorithm based on BP neural network proxy model and its application[D]. Changchun: Jilin University, 2021. (in Chinese)

[12] XIA Meng. Rapid trajectory optimization for flight vehicles with complex constraints[D]. Harbin: Harbin Institute of Technology, 2010. (in Chinese)

[13] YONG Enmi. Study on trajectory optimization and guidance approach for hypersonic glide-reentry vehicle[D]. Changsha: National University of Defense Technology, 2008. (in Chinese)

[14] HONG B, XIN W Q. Application of hp-adaptive pseudo-spectral method in rapid gliding trajectory optimization[J]. Computer Measurement & Control, 2011, 20(5): 948-953.

[15] QIU W J, MENG X Y. Multi-phase trajectory optimization of vehicle based on hp-adaptive pseudo-spectral method[J]. Journal of Beijing Institute of Technology, 2017, 37(4): 412-417.

[16] PATTERSON M A, RAO A V. GPOPS-Ⅱ: A Matlab software for solving multiple-phase optimal control problems using hp-adaptive Gaussian quadrature collocation methods and sparse nonlinear programming[J]. ACM Transactions on Mathematical Software, 2010, 41(4): 1-37.

Authors Mr. **LI Chang** received the B.S. and the M.S. degrees from Shanghai Maritime University in 2017 and Nanjing University of Aeronautics and Astronautics in 2023, respectively. He is currently a project manager at Marine Design and Research Institute of China. His research interests are flight vehicle design and project management.

Dr. **ZHAO Jisong** received the B.S. and Ph.D. degrees in Northwestern Polytechnical University in 2007 and 2012, respectively. He is currently an associate professor in Nanjing University of Aeronautics and Astronautics. His main research interests are flight vehicle design and optimization.

Author contributions Mr. **LI Chang** contributed to the simulation results and wrote the manuscript. Dr. **ZHAO Jisong** designed the study and improved the quality of the manuscript. Both authors commended on the manuscript draft and approved the submission.

Competing interests The authors declare no competing interests.

(Production Editor: LIU Yandong)

变构型高超声速滑翔飞行器再入轨迹优化

李 畅, 赵吉松

(南京航空航天大学航天学院,南京 211106,中国)

摘要:研究了变构型飞行器(Variable-configuration vehicle,VCV)的再入轨迹优化问题,建立了气动代理模型,用于快速预测不同变形和飞行条件下飞行器的空气动力学特性。以变形量、迎角和倾斜角的变化过程作为轨迹优化变量,定量研究了VCV的着陆区覆盖能力和避障机动性能。仿真结果表明,与固定配置飞行器(Fixed-configuration vehicle, FCV)相比,VCV除了可以实现沿再入-滑翔轨迹的最优控制之外,还可以沿再入轨迹进行最佳变形,从而达到更优的再入轨迹性能。

关键词:高超声速滑翔;气动代理模型;轨迹优化;可变构型